

Neural Memory Decoding with EEG Data and Representation Learning

Glenn Bruns Michael Haidar Federico Rubino
California State University, Monterey Bay
Seaside, CA 93955

Abstract

We describe a method for the neural decoding of memory from EEG data. Using this method, a concept being recalled can be identified from an EEG trace with an average top-1 accuracy of about 78.4% (chance 4%). The method employs deep representation learning with supervised contrastive loss to map an EEG recording of brain activity to a low-dimensional space. Because representation learning is used, concepts can be identified even if they do not appear in the training data set. However, reference EEG data must exist for each such concept. We also show an application of the method to the problem of information retrieval. In neural information retrieval, EEG data is captured while a user recalls the contents of a document, and a list of links to predicted documents is produced.

1. Introduction

Neural decoding is the reconstruction of stimuli or mental state from a record of electrical activity in the brain. An example is the reconstruction of an individual's emotional state (happy, sad, or neutral) from electroencephalogram (EEG) data. In the case of neural *memory* decoding, the problem is to identify a concept that is being recalled from a record of electrical activity in the brain. The problem is illustrated in Fig.1. Here we show it is possible, with high accuracy, to identify a concept being recalled using EEG data. It is assumed that a previously-recorded reference EEG recording is available for every concept to be recalled.

The neural memory decoding problem is important because of the light a solution can shed on the function of human memory. For example, consider the question of which frequency bands (alpha, gamma, etc.) are most associated with memory function. In a direct approach to understanding this relationship, one can examine brain data collected while a subject performs memory-related tasks. With a system for neural memory decoding, an alternative method can be used in which the accuracy of memory de-

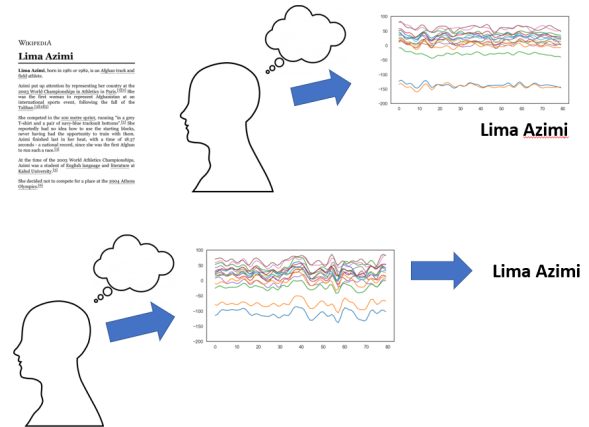


Figure 1. A problem of neural memory decoding. **Top:** An individual reads about a concept. Brain activity is recorded and labeled with the concept name. **Bottom:** Later, the individual recalls the concept. Brain activity is collected and used to identify the concept.

coding is compared across multiple data sets, each collected from a different set of frequency bands. Similarly, to help understand which regions of the brain are associated with memory function, one can compare the accuracy of memory decoding across data sets containing data from different EEG nodes.

The neural memory decoding problem is also important because a solution to the problem would enable useful applications. For example, a neural memory decoding system could be used for *neural document retrieval*, in which a user retrieves a previously-read document by simply thinking about it.

Solving the neural memory decoding problem is challenging. Brain structure changes over time. The brain activity associated with recalling something today will be different than recalling it tomorrow. Also, memory is a complex mental activity involving multiple cognitive functions and regions of the brain. Recalling a concept does not involve a

simple, localized pattern of brain activity.

Another challenge in solving the problem of neural memory decoding is in the experimental design and data organization. For each of many concepts, brain data must be recorded at multiple time points. Predicting a concept being recalled involves relating data recorded at the time of recall to data recorded at an earlier time. Additionally, while EEG recording devices are preferred for cost-effective experimentation, they suffer from noise and limited spatial resolution in comparison to more expensive alternatives like Functional Magnetic Resonance Imaging (fMRI).

In this paper, we demonstrate the feasibility of solving the neural memory decoding problem. Our data set consists of EEG traces from a single subject for 103 concepts. For each concept, EEG data was recorded while the subject recalled the concept at three points in time: immediately after the concept was learned, one day after the concept was learned, and 3 days after the concept was learned.

Our system correctly identifies the concept the subject recalls on day one with about 78.4% accuracy, on average, when trained on EEG traces for 78 concepts and tested on EEG traces for 25 concepts. An average accuracy of only 4% would be achieved by chance. Our system achieves a top-3 accuracy (the correct concept is among the top three predicted concepts) of about 94.4% (versus 12% by chance).

In operation, our system takes as input a 16-channel EEG trace recorded on day 1 and produces as output the concept name. The system is a deep neural net. It predicts the concept of a trace by segmenting the input EEG trace, mapping each EEG segment to a point in a compact representation space, predicting the concept of each point, and then combining these predictions to obtain a concept for the EEG trace as a whole.

The use of representation learning allows the concept of an EEG trace to be predicted even if no EEG trace with that concept was seen during the training of the system. This property is important in using the system for applications such as neural document retrieval. In this application, no new training is needed to classify a new concept.

In experiments that test system performance on data sets containing only a subset of the EEG nodes or frequency bands, we found that the left frontal and central nodes provided the highest trace classification accuracy of all individual nodes, and that the theta and gamma frequency bands provided the highest trace classification accuracy among all individual frequency bands.

Summarizing our main contributions, we have defined a problem of neural memory decoding with EEG data. We have developed a system that achieves top-1 concept prediction accuracy of about 78.4% when used on EEG data recorded when recalling a concept one day after it was learned. We have used our system to measure the predic-

tive power of individual EEG nodes and frequency bands.

2. Related work

Advancements in neuroimaging technology and computing have accelerated work in predicting the stimuli responsible for neural activity. fMRIs have emerged as the preferred method for investigating semantic decoding, a process that seeks to discern an individual's thoughts, but not necessarily memories. fMRI surpasses EEG in spatial resolution and functional detail, with neural patterns showing greater spatial distinctiveness compared to temporal characteristics. Additionally, EEG has a lower signal-to-noise ratio (SNR). However, machine learning and deep learning offer significant improvement in feature extraction, enabling scientists to effectively enhance the SNR and overcome the inherent low SNR associated with EEG data. [1]. Higher SNR is desired for lower levels of background noise. EEGs have also demonstrated comparable effectiveness in neural decoding, as shown by their ability to identify the subject of photos pertaining to either land mammals or tools [2, 3]. These two studies provide evidence of category-specific oscillatory patterns during semantic processes. However, unlike in this work, neither used deep learning nor did they explore multi-day semantic memory.

Several studies demonstrate machine learning's ability to decode cognitive functions from neural activity recorded via EEG. Emotion recognition, which seeks to identify emotional states [4–8], has applications ranging from clinical research [9] to targeted product development [10, 11]. Other studies involving neural decoding via EEG and machine learning involve motor tasks and motor imagery [12–18], seizure detection [19–22], mental workload [23, 24], and even visual stimulus decoding [25, 26].

Semantic neural decoding attempts to interpret meaningful information from neural activity associated with language, semantic associations, and meaning-related stimuli. The underlying cognitive mechanisms involved in understanding and representing meaning are of particular interest. For example, neural activity patterns exhibit similarities when contemplating pictures and words belonging to the same category, providing evidence of unique neural patterns associated with semantic concepts combined with visual stimuli [27]. Semantic concepts, such as faces, locations, and objects also have distinct neural patterns that persist between a study and recall phase [28]. This lends support to reinstatement theory, a memory model in which recall occurs through reactivation of cortical patterns specific to a memory [29], and implies that memories can be discriminated categorically. Distinct neural signatures have been demonstrated for abstract concepts such as *multiplication* and *consciousness* [30]. Using fMRI, participants' brain activity was recorded during contemplation of 28 abstract concepts and subsequently during the recall of pre-

viously studied properties. Discrimination of neural signatures was observed across abstract concepts.

Less common is work on the neural decoding of memory. A theoretical division of memory separates memory into two sub-types. Episodic memory consists of memory involving events or episodes in a person’s life, whereas semantic memory consists of general knowledge or facts [31]. The creation and retrieval of semantic memories is dependent on language processing, working memory, and other phonological processes [32].

Some previous work has decoded EEG data of episodic memory. In [33], a classifier was developed to predict the category of a photograph based on EEG data recorded during the encoding of an episodic memory involving a photograph and a paired word. Each photograph belonged to one of three categories: landscape, face, or object. Different authors, using the same data set as in [33], achieved a classification accuracy of 0.74 on the same problem using a Morlet transform network [34].

fMRI data and multi-voxel pattern analysis (MVPA) have also been used to classify episodic memories. In one study faces were classified as new (unseen) and old (seen) faces [35]. Researchers collected data while participants identified whether pictures of faces had been previously studied and successfully decoded explicitly identified faces as new or old, showing individual episodic memories are detectable using neural decoding of memory states. The study was later expanded to include 180 scenes of participants’ daily life. fMRI data was again collected, this time participants were asked to categorize a captured video image into six different levels of familiarity from “confidently not their experience” to “perfect recollection of experience”. The researchers used MVPA to classify between the six recollection statuses with .35 accuracy [36].

The work described in this paper differs in three main ways from the aforementioned studies. The first difference is the time at which the training data was collected. Our data was collected across multiple days following a study period on the first day. The spread of recordings across different days increases the variability of the EEG data, resulting in a more challenging classification task. Multi-day data tests the ability of convolutional neural networks (CNNs) to decode neural signals used to access (concept-specific) content stored in memory while representing a more realistic application of brain-computer interface (BCI) information retrieval. Second, both our training and testing data were of cued semantic recall (information was presented to cue a memory), there was no verbal response. Whereas [33] and [34] used pairs-associates encoding data recorded during the study phase as training data and tested on image-cued verbal recollection data. While there is evidence that encoding and recollection processes of memory co-vary [37], particularly in hippocampal activation and cortical reinstatement

[38], studies able to observe such phenomena historically employ more sophisticated equipment such as fMRIs [38–41]. Third, our system uses CNNs, which are distinct from MVPA. CNNs are a class of deep learning models designed to learn hierarchical representations of data through convolutional layers. MVPA is a computational method primarily used to analyze patterns of neural activity across voxels, three-dimensional representations of a specific location within the brain, typically from an fMRI. A voxel contains information on intensity level or neural activity measured at a particular location.

To our knowledge, no previous study has achieved neural decoding of semantic memory using EEG and deep learning. Beyond semantic memory decoding, deep learning has increasingly been used for other neural decoding tasks. Deep learning with a transformer architecture has been used to classify five stages of sleep through EEG representation learning [42]. The authors use self-supervised learning with loss measured between raw EEG input and reconstructed signals from masked features (reconstruction loss), while we use supervised contrastive loss.

Multi-modal models have been used in sentiment analysis and relation detection for natural language processing [43]. The authors decoded EEG representations using both EEG and eye tracking data. Other recent work in neural decoding and classification using deep learning focuses on working memory [44,45], sleep state levels [46,47], and abnormality detection [46, 47]. A few studies have also used multi-input models to work across multiple paradigms such as imaginary movement, visually evoked responses, movement-related cortical potential, and error evoked responses [14,48].

3. Background

Machine learning has increasingly been used to analyze physiological signals such as heart rate, blood pressure, electrocardiography, and EEG [14, 49, 50]. BCIs harness mental activity, often measured via EEG, to directly control a range of devices from prosthetics to computers [51]. This mental activity originates from cognitive functions and creates measurable voltage fluctuations across the brain, the result of billions of neuronal events.

EEG measures the frequency at which neuron potentiation rises and falls - referred to as neural oscillations or brain waves - during brain activity. These brain waves give insight into the communication between neurons and reflect cognitive, and sensory, mental processes [52]. EEG devices read these measurements via electrodes placed across the scalp. Each electrode (channel) measures the frequency of brain activity at its location. A standard analysis of brain activity uses frequency bands (rates of oscillations) - delta (1–3 Hz), theta (4–7 Hz), alpha (8–12 Hz), beta (13–30 Hz), gamma (30–100 Hz) - and their observed locations [53].

Types of brain activities observable with EEG include processing of information that results in alpha-band oscillations [54]. Other cognitive tasks, such as generation and rehearsal of speech from verbal working memory, produce theta frequencies in both ventral-frontal and left parieto-temporal areas of the brain [55]. Similar areas are also activated during cued recall of explicit memory (memories of facts) [56]. Despite an established understanding of frequencies and topology, the high intra-subject variability of brain activity has plagued EEG studies [57].

Other methods of investigating brain activity include functional magnetic resonance imaging (fMRI), positron emission tomography (PET), magnetoencephalography (MEG), and functional near-infrared spectroscopy (fNIRS). Currently, only fNIRS and EEG provide the temporal resolution, cost-effectiveness, and portability desired in a BCI system. For our purposes, EEG was selected for its cost and wealth of relevant literature.

4. Data collection and preprocessing

4.1. Data Collection

Raw data was collected with OpenBCI’s Ultracortex Mark IV Headset, Cyton board, Daisy module, and GUI software (version v5.0.0). EEG data was sampled at 125 Hz using 16 channels organized in the 10-20 system with a referential montage. The earlobe was used as an online reference signal.

150 Wikipedia [58] pages were selected by one of the paper’s authors and arranged into groups of size 10. The topics were chosen to be neither too obscure nor too familiar. Many concern people (e.g., Luisa May Alcott, Alan Greenspan), places (e.g., Dublin, Great Barrier Reef), and ideas (e.g., portrait, tangram). In what follows, Wikipedia page topics are referred to as *concepts*.

A second author then read the pages and recorded EEG data. Each recording session involved one group of concepts. The day 0 recording session was structured as follows. First, the Wikipedia pages for the concepts in the group were studied for five minutes each. Then, for each concept:

- The subject was cued with the concept.
- The subject was recorded for 75 seconds recalling the main points of the page.

The day 1 recording session took place the following day and had the same structure as the day 0 session. The day 3 recording session took place two days after the day 1 recording session and had the same structure as the day 0 session.

The recordings for 47 pages were dropped because of data quality issues, leaving recordings for 103 pages, which are listed in Appendix A.

4.2. Preprocessing

We refer to the EEG data collected for one concept at a single sitting as a *trace*. Each raw trace was preprocessed using the following sequence of operations:

Clipping. Sample values outside the range defined by the 0.005 and 0.995 quantile values (computed for the trace as a whole) are replaced by the range limit values. This process is also known as “clamping”.

Occipital Noise Removal. For each channel, at each time step, the sample value of the channel is reduced by the sample value of the occipital channel, ipsilaterally. The left occipital channel serves as the new reference for the left-hand channels, and similarly for the right-hand channels. The occipital channels are then removed from the trace, leaving 14 channels.

While other re-referencing methods appear in the literature, there is no definitive method for increasing memory signal, a process of removing unwanted noise from EEG data containing memory information. The occipital electrodes (O1, O2) are closest to Brodmann’s area 17/18 corresponding to the visual cortex and are thought to carry more noise from the visual network [59,60]. Re-referencing with the occipital nodes allows for stronger signals recorded at regions of the brain associated with memory (see Section 6.3).

Frequency filtering. A FIR bandpass filter is applied to retain data only in 1-100 Hz range, which includes the delta, theta, alpha, beta, and gamma frequency bands.

Normalization. Each channel in the trace is independently normalized using z-score normalization, so that the samples of the channel are zero-centered and have unit standard deviation.

Trimming. Finally, the first and last 4 seconds of the trace are removed. This step removes edge artifacts produced by the FIR filter and removes data recorded while the subject relaxes and begins focusing on a concept.

5. Method

Our system is a multi-class classifier that takes an EEG trace as input and produces a probability distribution over concept classes as output. Key features of the system are the use of representation learning, the treatment of data collected at different points in time, and the ensemble method used to classify EEG traces using predictions of the segments in the trace.

5.1. Overview

Predicting a concept class from an EEG trace involves the four steps shown from left to right in Fig. 2. First, the input trace is segmented using a sliding window, yielding a collection of segments. Each segment is then encoded by mapping it to a low-dimensional space. The concept class

of each segment is then predicted. In particular, for each segment, the probability of each concept class is computed. Finally, the predicted class of the trace as a whole is computed from the predicted classes of the trace’s segments.

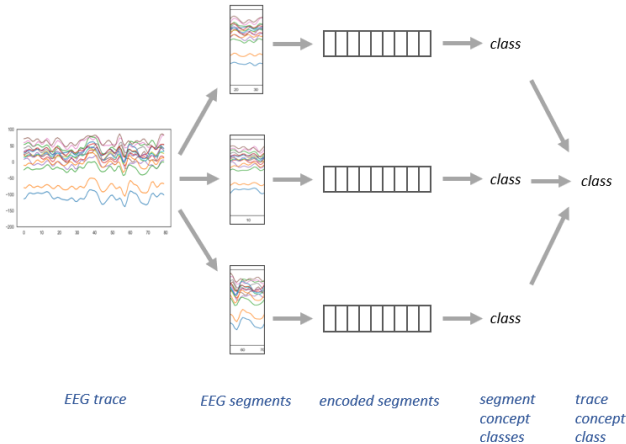


Figure 2. The trace classification process. The input EEG trace is segmented and then each segment is encoded and classified. The resulting concept classes are combined to identify a concept class for the trace as a whole.

This method, in which the encoding of an input is performed independently from downstream tasks such as classification, is called *representation learning* [61].

Fig. 3 illustrates the encoding of the segments of a trace to the lower-dimensional embedding space. In the figure, the points in the embedding space are colored according to the concept associated with each trace. The segment encoder is trained using segments from a set of training traces; its goal is to map segments from the same trace to nearby points in the embedding space, and segments from distinct traces to distant points. (The figure is simplified in that it does not show the preprocessing that is applied to segments before they are mapped to the embedding space.)

There are several benefits to using representation learning in segment classification. First, segment classification can be performed even for classes never seen during the training of the segment encoder. Second, the learned representation of segments can be used to solve problems other than segment classification. Third, one can hope to gain an understanding of the important features of EEG segments by studying the learned embedding space.

The concept class of a trace is then predicted by combining the predicted classes of the segments in the trace. For each class, the predicted probabilities of the class across all segments are summed and then normalized to obtain a probability distribution over concepts.

The main components of our system are the *segment encoder*, which maps segments to their encodings, the *segment*

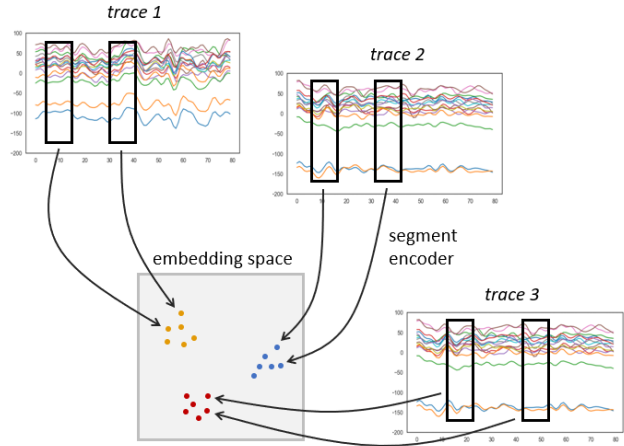


Figure 3. The embedding of segments of EEG traces into a lower-dimensional space.

classifier, which predicts the concept class of an encoded segment, and the *trace classifier*, which predicts the concept class of a trace as a whole. In the following sections these system components are described in detail.

Because the brain activity associated with the recall of a concept changes over time, special attention is paid to how EEG traces recorded on different days are used to train and evaluate the system (see Fig. 4). Concepts are first split into a set of training concepts and a set of test concepts. In training the segment encoder, for each training concept, traces from day 0 and later days are used. In this way, the segment encoder can learn what is invariant in the EEG data recorded when recalling at multiple points in time. In training the segment classifier, traces from only day 0 are used. In testing, trace concept predictions are made for traces recorded after day 0.

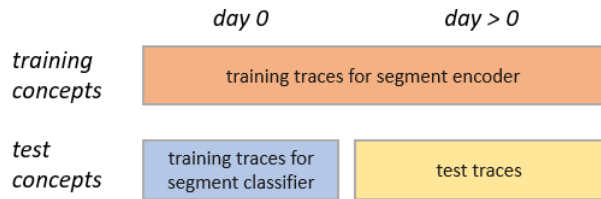


Figure 4. Organization of the system’s training and test sets.

5.2. Data segmentation

The preprocessed EEG traces are segmented using a window size of 100 samples with an offset (or “stride”) of 10 samples, giving a segment length of 800 ms. In segmenting the traces we are relying on the stationarity of EEG data, at

least insofar as concept recall is concerned. Whether EEG data should be regarded as stationary is the subject of disagreement in the literature [62, 63].

Each segment is then independently preprocessed using the following sequence of operations.

Trend removal. A heuristic method is used to detect trend in segments. For each channel in a segment, the trend of the channel is computed as the absolute difference between the means of the first and second halves of the segment. The trend for the segment as a whole is then computed as the maximum of channel trends. The 5% of the segments for a concept that most display trend are dropped.

Outlier removal. An anomaly detection algorithm is used to identify the most anomalous segments of each concept, which are then dropped. For the purpose of anomaly detection, each segment is mapped to a feature vector by taking the standard deviation of each channel separately. These feature vectors are then provided as input to the isolation forest anomaly detection algorithm [64]. The output scores from the algorithm are used to rank the segments, and the 5% of the segments deemed most anomalous are dropped.

Normalization. Finally, each segment is normalized by applying z-score normalization independently to each channel of the segment.

5.3. The segment encoder

The segment encoder maps EEG segments to encodings in the embedding space.

5.3.1 Neural architecture

Fig. 5 shows the architecture of the segment encoder. Processing stages are shown on the left; the dimensions of the data between stages are shown in the blue boxes. The encoder input is an EEG segment. In the first stage of processing, convolution and max pooling are applied. The convolution operation has 256 filters of size 3. Conceptually, each filter is passed over all 14 channels of segment data, producing a single new time series of about the same length as the input segment. Combining the output from each of the filters yields a time series of 256 channels. The output of the convolution operation is passed to a max pooling operation of size 2 and stride 2, which has the effect of reducing the number of steps in the time series.

After several convolution and pooling blocks are applied, a convolution operation is followed by global max pooling, which outputs the maximum value found in each channel, yielding a time series of length 1. A flattening operation then transforms the time series into a vector of length 256. Informally, these stages of convolution and pooling operations extract 256 features from the input segment. The use of global max pooling is consistent with our assumption that

the EEG data is roughly stationary; after global max pooling the temporal dimension of the input data is absent.

The vector of length 256 is then processed by several fully-connected neural layers, resulting in a final encoding of size 32. Overall, the encoder maps a segment from an input space of 100×14 dimensions into embedding space of just 32 dimensions. The neural encoding model itself has 655,136 parameters. The values of the parameters are determined by the training process.

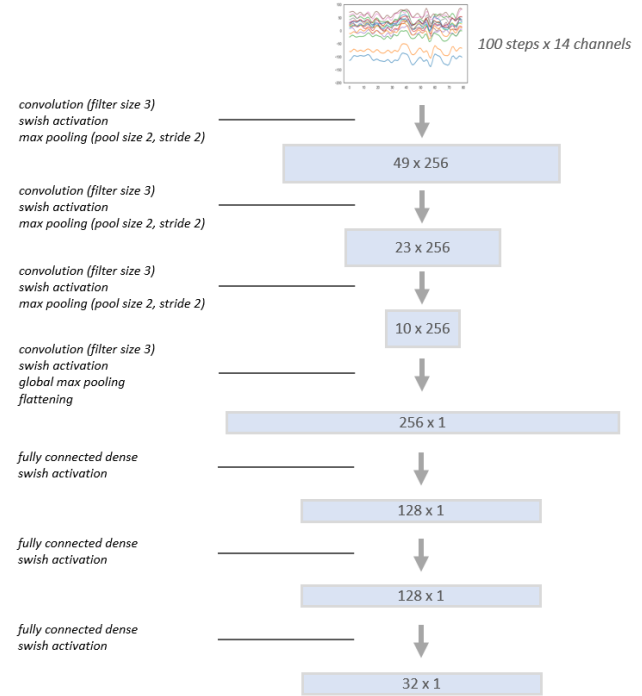


Figure 5. Architecture of the segment encoder.

5.3.2 Loss function

The loss function used to train the segment encoder is supervised contrastive loss [65]. With this function, the loss value for a batch of training examples is low if the segments associated with the same concepts are nearby in the encoding space, and the segments associated with different concepts are widely separated in the encoding space. In other words, the goal of supervised contrastive loss is an encoding space in which the segments associated with a concept form a cluster in the encoding space.

Khosla *et al* (see [65], equation 2) define the supervised contrastive loss \mathcal{L} for a set of embeddings as shown below. The set of embeddings and corresponding labels is $\{(z_i, y_i) \mid i \in I\}$ (where I is an index set), $A(i)$ is the set of all indexes in I except i , and $P(i) = \{j \in A(i) \mid y_j = y_i\}$ is the set of indexes of embeddings with the same label as

z_i , but not including i . The definition is parameterized by variable τ , the “temperature” parameter.

$$\mathcal{L} = \sum_{i \in I} \frac{-1}{|P(i)|} \sum_{p \in P(i)} \log \frac{\exp((z_i \cdot z_p)/\tau)}{\sum_{a \in A(i)} \exp((z_i \cdot z_a)/\tau)}$$

The definition assumes the embeddings have been $L2$ -normalized. In other words, the length of each embedding is 1 when the length is measured using Euclidean distance. Because the embeddings are $L2$ -normalized, the dot product of two embeddings equals the cosine of the angle between them; the “cosine distance”.

Intuitively, the definition states that the loss for an embedding is based on the average similarity of the embedding with other embeddings of the same class. Operationally, the loss for a single embedding z_i can be computed as follows. First, use the dot product to compute the similarity of z_i and every other embedding z_a . Second, normalize the similarity values by dividing them by their sum. Third, compute the log of each normalized similarity. Finally, get the average of these log similarity values for embeddings of the same class as z_i , and negate it.

Supervised contrastive loss was originally defined [65] in the context of image classification and a learning framework that includes not just an encoder but also data augmentation and a “projection head”. The data augmentation component produces two modified images from a single input image. The projection head is a feedforward neural network with only one or two layers. In training, the output of the encoder is fed to the projection head. After training, the projection head is not used.

In our model, the projection head is a feedforward neural network with two layers, each of 64 neurons. Data augmentation in the style of [65] is not used. We use a variant [66] of the definition of supervised contrastive loss shown above. In the variant, the definitions of $P(i)$ and $A(i)$ are modified so that both $P(i)$ and $A(i)$ are extended to include i itself. In other words, the similarity of i with itself is included in the loss value. We use a temperature parameter value of 0.1.

5.3.3 Training

Training of the segment encoder proceeds in steps. In each step, the encoder is given a set of segments, called a *batch*. In cost functions used with one-shot learning, system performance can depend strongly on how training examples are selected for each batch. In representation learning with supervised contrastive loss, experiments suggest that accuracy improves with larger batch size [65]. In our system, each batch contains 8 segments for each training concept, giving a batch size of 78×8 segments. Batches are generated on-the-fly with a batch generation function.

To reduce model overfitting, zero-centered Gaussian noise is added to each segment, with variance controlled by

a system tuning parameter. Training proceeds for 8 epochs, each having 500 steps. An rmsprop [67] optimizer is used.

Fig. 6 shows the embedding of about 1000 random segments after training the segment encoder. The embeddings, of length 32, have been mapped to 2-dimensional space using t-distributed stochastic neighbor embedding (tSNE) [68]. Each point represents a segment and is colored according to the Wikipedia page concept it is associated with. The legend lists only some of the concepts contained in the training data set.

Fig. 7 shows the embeddings of segments associated with concept classes not seen during the training of the segment encoder. As in Fig. 6, the embeddings have been mapped to 2-dimensional space using tSNE. Even though these concept classes were not seen during training, the segments cluster well in the embedding space according to the concepts.

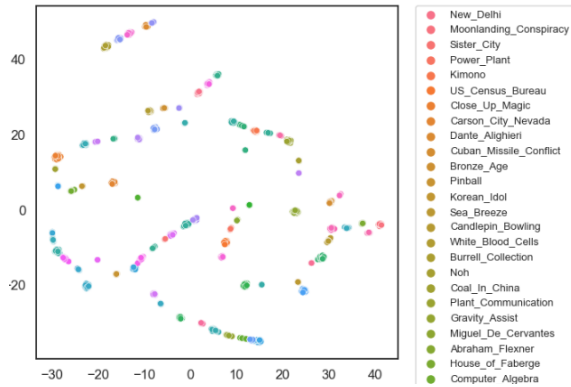


Figure 6. Embeddings of training segments after mapping to two dimensions.

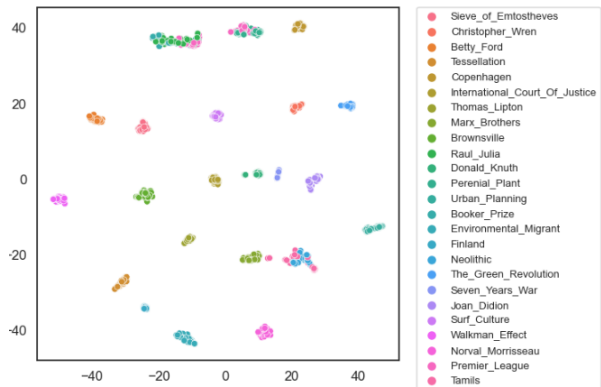


Figure 7. Embeddings of test segments after mapping to two dimensions.

5.4. The segment classifier

The segment classifier takes an encoded EEG segment as input and outputs a concept class. Any machine learning algorithm can be used to create the segment classifier. We use a k-nearest-neighbors (KNN) classifier with 25 nearest neighbors, and Euclidean distance as the distance function.

Our KNN classification method supports predictions in the form of a probability distribution over the concept classes. In other words, the prediction function takes as input an EEG segment and outputs a probability distribution over concept classes. KNN classification is a form of instance-based learning, in which the training data itself serves as the model, and therefore the training process involves only storing the training data.

5.5. The trace classifier

The trace classifier takes an EEG trace as input and outputs a probability distribution over concept classes. It is an ensemble classifier that predicts the concept class of a trace from the predictions of concept classes in the segments of the trace.

The trace classifier first preprocesses and segments the input trace (as described in Section 5.2), then applies the segment classifier to classify each segment. Because the segment classifier’s output for each input segment is a probability distribution over concept classes, a “soft” method is used to combine the segment predictions to form a prediction for the trace as a whole. For every concept class, the predicted probabilities for the class across all segments are summed. The resulting vector of sums is then normalized to obtain a probability distribution over the concept classes. The trace classifier needs no training of its own.

6. Results

Here we describe our experimental setup and experimental results. Our experiments attempt to answer two broad questions. First, what is the performance of our system in predicting the concept class of an EEG trace? Second, what can our system tell us about the brain’s memory function?

6.1. Experimental setup

To test our system we perform a number of experimental trials, where a single trial consists of the following steps: (Recall that our data set contains EEG traces for 103 concepts.)

1. A test/train split is performed. 25 concepts are randomly selected, and segments for these concepts are put in a test set. Segments for the remaining concepts are put in a training set.
2. The segment encoder is trained on batches from the training set.

3. A KNN classifier is created using the day 0 segments from the test set as training data.
4. Concept predictions are made by the KNN classifier on day 1 segments from the test set. Top-1, top-2, and top-3 accuracy values are computed using the concept labels of the test set.

Running multiple experimental trials on the system yields a set of accuracy values with high variance. One source of the variance is the random initialization of weights in the training of the source encoder. Another is the random split of the concepts into training and test sets. Also, every trial contains only 25 concepts, so the resulting accuracy for the trial will be a value in $\{0.0, 0.05, 0.10, \dots, 1.0\}$.

Variance in experimental results makes the evaluation of system performance difficult, which in turn makes system tuning difficult. To address this problem, 25 trials are run, and then the bootstrap is used to compute a confidence interval for accuracy values.

This approach, in which multiple trials are run, each with its own randomly-chosen test/train split, is a variant of cross-validation. In cross-validation, a set of training examples is randomly split into n disjoint groups, called *folds*, and then a training and test process is performed n times. Each time, a distinct fold is used as the test set, and the remaining folds are combined for use as the training set. We cannot use simple cross-validation because we want training and test sets to contain segments of different concepts. We do not simply split the concepts into n folds because then larger values of n lead to folds containing a small number of concepts, which makes the test results unreliable. By splitting the concepts into random groups instead of n disjoint folds, we can separately control the number of trials and the number of concepts represented in a test set.

In reporting test results, we provide the mean top-1 and top-3 accuracy values across all trials in a test.

6.2. Trace and segment classification accuracy

Trace classification accuracy. The most important performance statistic for our system is the trace classification accuracy: the accuracy in predicting a concept given an EEG trace of the subject thinking of the concept.

Our system achieves a mean top-1 validation accuracy of 78.4%, and a top-3 validation accuracy of 94.4%. Our test set contains 25 concepts, with 1 trace for each concept, so our top-1 accuracy of 78.4% can be compared to a baseline of 0.04 that could be achieved by chance. Similarly, our top-3 accuracy of 94.4% can be compared to a baseline of 0.12. These top-1 and top-3 accuracy values were achieved on concepts that were not used in the training of the segment encoder.

Figure 8 shows our overall performance results, based on 50 trials. The error bars in the figure represent a 95%

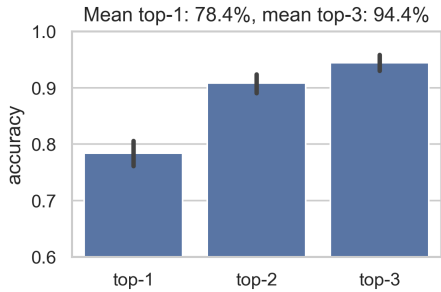


Figure 8. System trace classification accuracy.

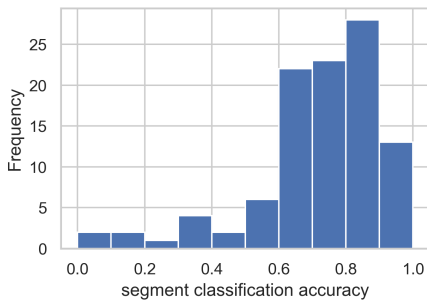


Figure 9. Histogram of per-concept classification accuracy.

confidence interval obtained by using the bootstrap on the accuracy values from individual trials.

Segment classification accuracy. The trace classifier uses predictions on many individual segments to make its own prediction. What accuracy is achieved by the segment classifier on a single segment? To evaluate segment classification performance, 50 trials were performed using our baseline hyperparameter settings. In each trial, classification was performed on all of the day 1 test segments. In all, about 1.06 million segments were classified; on average about 10,300 classifications per concept.

An overall segment classification accuracy of 0.725 was obtained, versus 0.04 by chance. However, accuracy varied significantly by concept. Figure 9 shows the distribution of the per-concept accuracy values. For some concepts, the segment classification accuracy is above 90%, while for others, it is below 10%.

Per-concept segment classification accuracy varies not just across concepts, but also across trials. In each trial a different, random split of concepts into training and test concepts is used. The train/test split controls which concepts are used to train the segment encoder, and the set of test concepts that must be distinguished in testing.

Fig. 10 shows how per-concept segment classification accuracy varies across trials. The plot on the left shows the mean accuracy across trials for the concepts with the high-

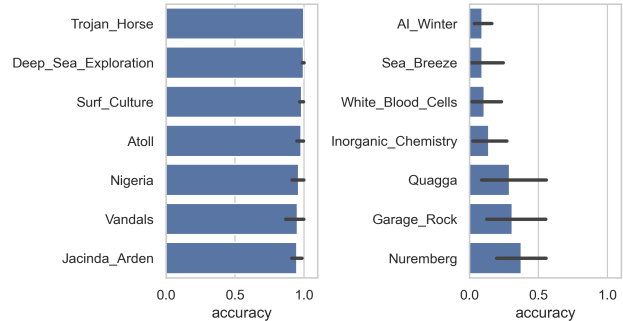


Figure 10. Average concept classification accuracy for concepts with high average accuracy (left) and low average accuracy (right).

est mean accuracy, while the plot on the right does the same for the concepts with the lowest mean accuracy. 95% confidence intervals obtained by bootstrapping are also shown.

The figure shows that some concepts, such as “Algebraic Structure”, achieve near-perfect segment classification accuracy in every trial in which they appear, while others, like “Bohemianism”, achieve very low accuracy across trials. The segment classification accuracy for concepts like “Kimono” and “Inorganic Chemistry” shows high variance across trials – and thus depends on the concepts used for training.

6.3. EEG node and frequency importance

Here we look at the predictive power of individual EEG channels and EEG frequency bands. For example, we look at the trace prediction accuracy that can be obtained if the EEG data only contains data from the F3 node.

Predictive power of EEG channels. Fig. 11 shows the average trace prediction accuracy obtained when trained and tested with data from only a single EEG channel. Here, “average” means the average of the top-1, top-2, and top-3 trace accuracy values. For example, a version of our data set was created containing only data from the F3 node. No tuning of our system was performed to optimize its accuracy with this data set; hence, the accuracy values shown in the figure are conservative.

The figure shows that the F3 node provides the highest predictive power of any node taken alone, with an average accuracy of about 0.28. Next in predictive power are the Fp1, C4, and C3 nodes. The nodes with the lowest predictive power are the F4, Fp2, and T6 nodes. The occipital nodes are left uncolored because occipital data is removed during preprocessing.

While EEG may not have the spatial resolution offered by fMRI, PET, or ECoG, the predictive power of specific EEG channels correlates with known brain functions and their regions within the brain. Channels C3 and F3 cover

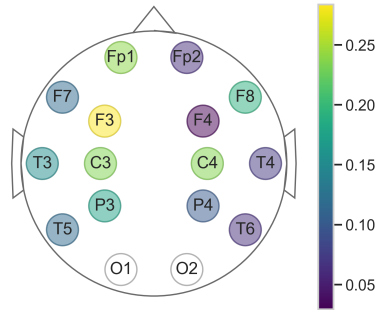


Figure 11. Average trace classification accuracy using data from individual EEG nodes.

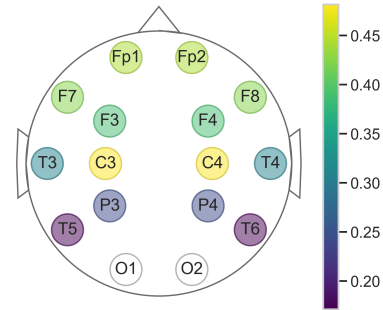


Figure 12. Average trace classification accuracy using data from pairs of EEG nodes.

the superior frontal gyrus. Activation in the left superior frontal gyrus has been linked to semantic categorization, the process of determining the class or group of a concept [69]. Channel Fp1 covers the left prefrontal cortex, which has long been linked to semantic processing, including semantic working memory [70].

Fig. 12 shows the average trace prediction accuracy for data sets from bilateral pairs of EEG nodes. The highest average trace accuracy of about 0.48 is obtained using the central nodes. We hypothesize this is due to their central location combined with low spatial resolution of the EEG. The nodes, located in proximity to the frontal cortex, encompass the angular and supramarginal gyrus, which have been linked to sentence processing [71], semantic memory [72], and various phonological processes [73]. Channels P3 and P4 scored half as well (0.242) as the central nodes. We speculate this reflects incomplete information of cortical reinstatement activity during a concept's retrieval.

The prefrontal (Fp1 and Fp2) and lateral prefrontal (F7 and F8) pairs show the second and third highest average trace accuracy, respectively. The Fp1 and Fp2 nodes cover the prefrontal cortex which is responsible for many functions; most relevant to this paper are goal direction and top-down memory retrieval [74]. The F7 and F8 nodes are expected to contain information from the medial and inferior frontal gyri, including Broca's area. These areas are known to play key roles in semantic retrieval and working memory [75].

Fig. 13 shows the predictive power of the nodes in the left and right hemispheres taken on their own. The nodes of the left hemisphere have higher predictive power than the nodes of the right. The average accuracy for the left is about 13% better than the average accuracy for the right. These results are consistent with research showing asymmetrical hemisphere activation during semantic processes, including memory [76–79].

Predictive power of EEG frequency bands. Figure 14 shows the top-1 concept prediction accuracy for EEG data

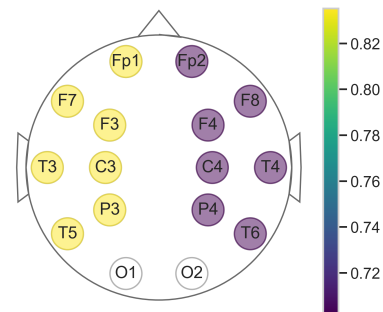


Figure 13. Average trace classification accuracy using data from nodes of the left and right hemisphere.

from single frequency bands. At least 20 trials were performed for each frequency band. Also shown is the concept prediction accuracy when all of the delta through gamma frequency bands are used. Trace classification accuracy as a function of frequency band serves two main roles: it provides validation of the cognitive functions being learned by our model and gives insight into the frequencies that contain information on the content of semantic memories.

Several studies have investigated the connection between memory and frequency bands. Memory-related coherence, a measure of synchronization between brain regions, has been seen within the lower frequencies (1-19 Hz) [80]. Delta and theta waves have also been linked to working memory and attention [81, 82]. Most significantly, gamma and theta bands, which produced the two highest accuracies among individual bands, show the most activity during semantic memory retrieval [83]. Decrease in alpha and beta oscillations is also well known to occur during memory tasks from attention to memory retrieval, for an in-depth discussion see [84]. Working memory, attention, and semantic retrieval are underlying cognitive functions potentially used to decode the content of a memory trace within our system.

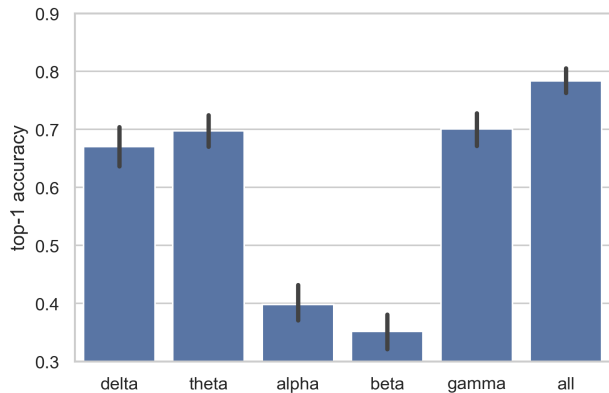


Figure 14. Top-1 trace classification accuracy by EEG frequency band.

6.4. Effects of recollection time

EEG data was collected when the subject recalled a concept just after learning it, one day after learning it, and three days after learning it. In section 6.2, we reported on our model’s accuracy in predicting a concept given EEG collected one day after learning it.

Figure 15 shows top-1, top-2, and top-3 trace prediction accuracy for days 1 and 3. Top-1 accuracy drops from about 0.7 to about 0.55, while top-3 accuracy shows a smaller decline, from about 0.95 to about 0.91.

We speculate the drop in accuracy between days reflects memory consolidation, the process by which, over time, memories are reorganized [85]. Observing which changes affect memory prediction could lead to a better understanding of memory consolidation and neural plasticity, a use case for our system. For example, testing for Alzheimer’s disease involves expensive MRI equipment to observe brain fluids, spinal taps to extract cerebral spinal fluid, or blood sampling and testing for amyloid proteins. We speculate that our system could lead to new indicators, such as the prediction accuracy delta between days, that signal for further, more invasive, testing. Similar applications may also be found in brain trauma, aging, and other, memory-related research.

7. Neural information retrieval

In this section we describe an application of neural memory decoding to information retrieval, and present experimental results pertaining to whether the application is practical.

The application would work as follows. A user encounters a document of interest. To *index* the document, the user briefly recollects the content of the document while EEG data is collected. The EEG trace for the document is stored

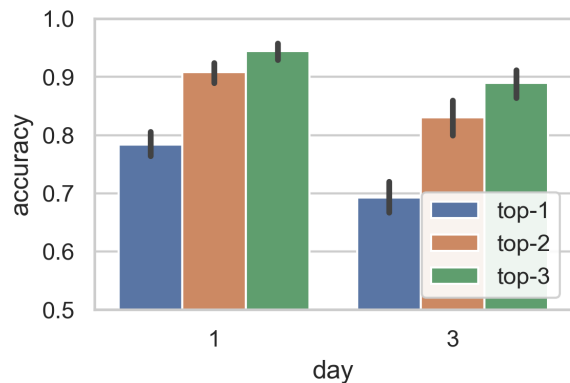


Figure 15. Accuracy by day of recollection.

along with a link to the document. Later, to retrieve the document, the user creates a *query* by again recalling the content of the document. The application then returns an ordered list of document links, ordered by estimated relevance. Only previously-indexed documents would appear in the list. Any kind of document could be used, provided it has a unique identifier, such as a URL. The document need not be a text document. It could be an image, an audio recording, or a video recording, for example.

Before using the system, the user would need to customize the system through a training process. In this process, the user would be asked to provide EEG data for a collection of short documents. For each document, the user would first read (or otherwise experience) the document, then record EEG data while imagining it.

This application addresses a pressing real-world problem. As more information becomes easily available through the internet, locating a document that one has previously discovered becomes more difficult. Solutions such as creating and storing bookmarks rely on user-created labels, which can be hard to create and provide little information about a document. EEG data of the recollection of a document, on the other hand, serves as an information-rich label.

Fig. 4 can be revisited in the context of this application, which we call “neural information retrieval”. The application would be trained using EEG traces for a set of training concepts recorded on day 0 and one or more later days. To index a document (day 0), an EEG trace for the document would be recorded and stored. (Recall that, with a KNN segment classifier, no computation is needed for training.) To query a document (day > 0), an EEG trace for the document would be recorded and then used as input to the trace classifier. This process is much like the process of our experimental setup, except that in the application a query could happen at any time after day 0.

Neural information retrieval would not be practical if

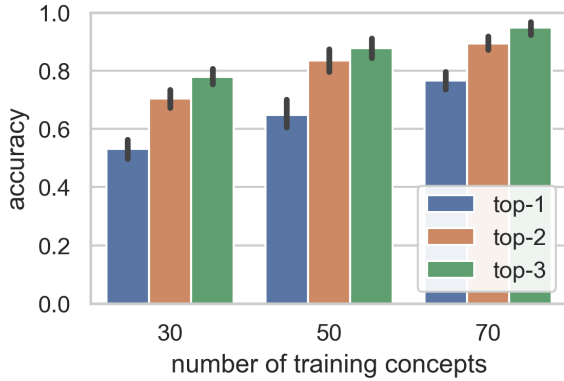


Figure 16. Accuracy by number of training concepts.

users would have to spend too much time collecting EEG data for system training, for indexing a document, or for searching for a document. The time to index and search for documents is most important, as training costs are incurred only once. We record EEG at 125 Hz, so a segment of 100 samples represents about 4/5 seconds. In other words, 10 segments can be recorded in about 8 seconds, even assuming the segments have no overlap.

Fig. 16 shows trace classification accuracy as a function of the number of concepts used to train the system. Data was collected from 20 trials, and all segments associated with each concept were used. Accuracy improves with the number of training concepts, but with 70 concepts the top accuracy values are about the same as is achieved with the full training set of 78.

Fig. 17 shows trace classification accuracy as a function of the number of training segments used per concept. All training concepts were used. Notably, only a small improvement is seen as the number of training concepts is increased from 20 to 320. No improvement is seen as the number of segments is increased from 320 to 640.

Fig. 18 shows trace classification accuracy as a function of the number of indexing and querying segments used. All training segments were used, and the number of indexing segments is equal to the number of querying segments. As the number of segments increases, top-1 accuracy increases, but there is a smaller improvement in top-3 accuracy. An average top-3 trace classification accuracy of about 0.94 can be obtained with 10 segments, compared to a value of 0.96 when 240 segments are used. On the other hand, the top-1 trace classification is about 0.56 with 10 segments, compared to 0.76 for 80 segments.

8. Conclusions

We have demonstrated the feasibility of neural memory decoding with EEG by creating a system that can pre-

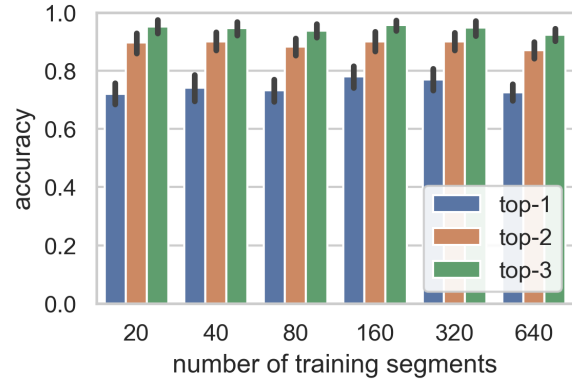


Figure 17. Accuracy by number of training segments.

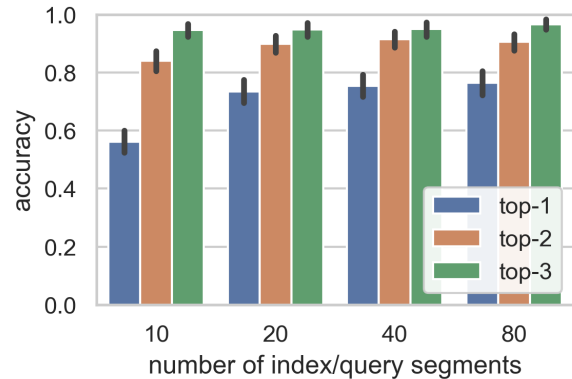


Figure 18. Accuracy by number of index/query segments. All training segments are used.

dict a concept being recalled with about 78.4% top-1 accuracy (4% chance) and about 94.4% top-3 accuracy (12% chance). One benefit of the work is the insight into memory function that can be obtained by studying how system performance varies as a function of the EEG frequencies that are used, the EEG nodes that are used, and the amount of data that is used. For example, we found that the single best EEG channel, in terms of concept prediction accuracy, was the F3 channel, and that the single best frequency band was the gamma band.

Another benefit of the work is the potential of the system in applications. We described a document retrieval application in which a user can retrieve a document by simply thinking about it. Our experiments shed light on whether this application might be practical in terms of the time a user would need to record EEG data when training or using the system.

Our system has serious limitations that need to be addressed, both for scientific reasons and to understand the

potential of neural memory decoding-based applications. First, our EEG data comes from just one individual. Second, for each concept, we collected data only over a 4-day period. Would our system perform well if a concept were recalled a month or a year after being first encountered?

Regarding future work, from a neuroscience perspective we would like to understand the features our convolutional model discovers in EEG data. Fortunately, many techniques exist for visualizing convolutional neural nets. For example, one can visualize the trained filters, or even superimpose a heat map on an input to see which regions of the input are most important to the classification process [86]. This could lead to new measures of memory consolidation or interference during recall.

Rapid advances are being made in the area of deep learning with neural nets. We would like to experiment with newer neural architectures, and to perform further system tuning to see how much our trace classification accuracy can be improved.

One can imagine many useful application of neural memory decoding. We would like to understand the practical issues associated with such applications, such as the amount of training data needed for a system that can distinguish thousands of concepts, the amount of indexing and query data needed, and whether reinforcement learning or other methods could be used to support applications that improve as they encounter more and more brain data.

The use of bulky, expensive EEG headsets may seem an obstacle to applications of neural memory decoding, but low-cost, comfortable EEG headsets for personal use are becoming available (e.g., the University of Oldenburg's cEEGrid [87]). We plan to experiment with such devices to see whether we can achieve results similar to those reported here.

An especially important issue to address in application of neural memory decoding is biometric data privacy. Today, the risk of sharing one's EEG data is not well understood. Applications using neural memory decoding can be designed in such a way that user EEG data never leaves a user's device. A potential benefit of using representation learning for neural memory decoding is that it opens the possibility of sharing with service providers only the encoded representation of a user's EEG data.

Acknowledgments

The work of Michael Haidar, and the equipment used in this project, was partly funded by the Undergraduate Research Opportunities Center (UROC) at California State University, Monterey Bay, the Koret Foundation, and the Office of the Director (OD) of the National Institutes of Health under grant number R25MD010391. The content is solely the responsibility of the authors and does not necessarily represent the official views of the National Institutes

of Health.

References

- [1] M. Rybář and I. Daly, "Neural decoding of semantic concepts: a systematic literature review," *Journal of Neural Engineering*, vol. 19, p. 021002, apr 2022.
- [2] B. Murphy, M. Poesio, F. Bovolo, L. Bruzzone, M. Dalponte, and H. Lakany, "EEG decoding of semantic category reveals distributed representations for single concepts," *Brain and language*, vol. 117, no. 1, pp. 12–22, 2011.
- [3] I. Simanova, M. Van Gerven, R. Oostenveld, and P. Hagoort, "Identifying object categories from event-related EEG: toward decoding of conceptual representations," *PloS one*, vol. 5, no. 12, p. e14465, 2010.
- [4] W. Ding and G. Marchionini, "A study on video browsing strategies," tech. rep., University of Maryland at College Park, USA, 1997.
- [5] J. J. Bird, A. Ekart, C. D. Buckingham, and D. R. Faria, "Mental emotional sentiment classification with an EEG-based brain-machine interface," in *Proceedings of DISP '19*, 2019.
- [6] Y. Yang, Q. Wu, M. Qiu, Y. Wang, and X. Chen, "Emotion recognition from multi-channel EEG through parallel convolutional recurrent neural network," in *2018 International Joint conference on Neural Networks (IJCNN)*, pp. 1–7, IEEE, 2018.
- [7] S. Rayatdoost and M. Soleymani, "Cross-corpus EEG-based emotion recognition," in *2018 IEEE 28th International Workshop on Machine Learning for Signal Processing (MLSP)*, pp. 1–6, IEEE, 2018.
- [8] J. Li, Z. Zhang, and H. He, "Hierarchical convolutional neural networks for EEG-based emotion recognition," *Cognitive Computation*, vol. 10, no. 2, pp. 368–380, 2018.
- [9] J. M. Mayor-Torres, S. Medina-DeVilliers, T. Clarkson, M. D. Lerner, and G. Riccardi, "Evaluation of interpretability for deep learning algorithms in EEG emotion recognition: A case study in autism," 2021. Preprint, arXiv:2111.13208.
- [10] Y. Liu, O. Sourina, and M. R. Hafiyandi, "EEG-based emotion-adaptive advertising," in *2013 Humaine Association Conference on Affective Computing and Intelligent Interaction*, pp. 843–848, IEEE, 2013.

- [11] M. J. Eugster, T. Ruotsalo, M. M. Spapé, O. Barral, N. Ravaja, G. Jacucci, and S. Kaski, "Natural brain-information interfaces: Recommending information by relevance inferred from human brain signals," *Scientific reports*, vol. 6, no. 1, pp. 1–10, 2016.
- [12] J. G. Cruz-Garza, Z. R. Hernandez, S. Nepal, K. K. Bradley, and J. L. Contreras-Vidal, "Neural decoding of expressive human movement from scalp electroencephalography (EEG)," *Frontiers in human neuroscience*, vol. 8, p. 188, 2014.
- [13] S. Kumar, A. Sharma, K. Mamun, and T. Tsunoda, "A deep learning approach for motor imagery EEG signal classification," in *2016 3rd Asia-Pacific World Congress on Computer Science and Engineering (APWC on CSE)*, pp. 34–39, IEEE, 2016.
- [14] R. T. Schirrmeister, J. T. Springenberg, L. D. J. Fiederer, M. Glasstetter, K. Eggensperger, M. Tangermann, F. Hutter, W. Burgard, and T. Ball, "Deep learning with convolutional neural networks for EEG decoding and visualization," *Human brain mapping*, vol. 38, no. 11, pp. 5391–5420, 2017.
- [15] Z. Tayeb, J. Fedjaev, N. Ghaboosi, C. Richter, L. Everding, X. Qu, Y. Wu, G. Cheng, and J. Conradt, "Validating deep neural networks for online decoding of motor imagery movements from EEG signals," *Sensors*, vol. 19, no. 1, p. 210, 2019.
- [16] M.-A. Li, Y.-F. Wang, S.-M. Jia, Y.-J. Sun, and J.-F. Yang, "Decoding of motor imagery EEG based on brain source estimation," *Neurocomputing*, vol. 339, pp. 182–193, 2019.
- [17] H.-L. Halme and L. Parkkonen, "Across-subject offline decoding of motor imagery from meg and EEG," *Scientific reports*, vol. 8, no. 1, pp. 1–12, 2018.
- [18] T. Sun, Q. Hu, P. Gulati, and S. F. Atashzar, "Temporal dilation of deep lstm for agile decoding of semg: Application in prediction of upper-limb motor intention in neurorobotics," *IEEE Robotics and Automation Letters*, vol. 6, no. 4, pp. 6212–6219, 2021.
- [19] P. Fergus, D. Hignett, A. Hussain, D. Al-Jumeily, and K. Abdel-Aziz, "Automatic epileptic seizure detection using scalp EEG and advanced artificial intelligence techniques," *BioMed research international*, vol. 2015, 2015.
- [20] A. Murugavel and S. Ramakrishnan, "Hierarchical multi-class SVM with elm kernel for epileptic EEG signal classification," *Medical & biological engineering & computing*, vol. 54, no. 1, pp. 149–161, 2016.
- [21] W. Mardini, M. M. B. Yassein, R. Al-Rawashdeh, S. Aljawarneh, Y. Khamayseh, and O. Meqdadi, "Enhanced detection of epileptic seizure using EEG signals in combination with machine learning classifiers," *IEEE Access*, vol. 8, pp. 24046–24055, 2020.
- [22] M. Savadkoobi, T. Oladunni, and L. Thompson, "A machine learning approach to epileptic seizure prediction using electroencephalogram (EEG) signal," *Biocybernetics and Biomedical Engineering*, vol. 40, no. 3, pp. 1328–1341, 2020.
- [23] F. Dehais, A. Lafont, R. Roy, and S. Fairclough, "A neuroergonomics approach to mental workload, engagement and human performance," *Frontiers in neuroscience*, vol. 14, p. 268, 2020.
- [24] Y. Zhou, S. Huang, Z. Xu, P. Wang, X. Wu, and D. Zhang, "Cognitive workload recognition using EEG signals and machine learning: A review," *IEEE Transactions on Cognitive and Developmental Systems*, 2021.
- [25] G. Shen, T. Horikawa, K. Majima, and Y. Kamitani, "Deep image reconstruction from human brain activity," *PLoS computational biology*, vol. 15, no. 1, p. e1006633, 2019.
- [26] Z. Jiao, H. You, F. Yang, X. Li, H. Zhang, and D. Shen, "Decoding EEG by visual-guided deep neural networks," in *Proceedings of the Twenty-Eighth International Joint Conference on Artificial Intelligence, IJCAI-19*, pp. 1387–1393, 2019.
- [27] M. Kumar, K. D. Federmeier, L. Fei-Fei, and D. M. Beck, "Evidence for similar patterns of neural activity elicited by picture- and word-based representations of natural scenes," *NeuroImage*, vol. 155, pp. 422–436, 2017.
- [28] S. Polyn, V. Natu, J. Cohen, and K. Norman, "Category-specific cortical activity precedes retrieval memory search," *Science (New York, N.Y.)*, vol. 310, pp. 1963–6, 01 2006.
- [29] J. D. Johnson, S. G. McDuff, M. D. Rugg, and K. A. Norman, "Recollection, familiarity, and cortical reinstatement: A multivoxel pattern analysis," *Neuron*, vol. 63, no. 5, pp. 697–708, 2009.
- [30] R. Vargas and M. A. Just, "Neural representations of abstract concepts: identifying underlying neurosemantic dimensions," *Cerebral Cortex*, vol. 30, no. 4, pp. 2157–2166, 2020.
- [31] E. Tulving, "Episodic and semantic memory," in *Organization of memory*, pp. 381–403, Academic Press, 1972.

- [32] M. Kutas and K. D. Federmeier, "Electrophysiology reveals semantic memory use in language comprehension," *Trends in cognitive sciences*, vol. 4, no. 12, pp. 463–470, 2000.
- [33] I. Bramão and M. Johansson, "Neural pattern classification tracks transfer-appropriate processing in episodic memory," *eNeuro*, vol. 5, no. 4, 2018.
- [34] O. Keding and D. Ohlin, "Statistics and machine learning for classification of emotional and semantic content of EEG," Master's thesis, Lund University, Sweden, 2021.
- [35] J. Rissman, H. T. Greely, and A. D. Wagner, "Detecting individual memories through the neural decoding of memory states and past experience," *Proceedings of the National Academy of Sciences*, vol. 107, no. 21, pp. 9849–9854, 2010.
- [36] J. Rissman, T. E. Chow, N. Reggente, and A. D. Wagner, "Decoding fmri signatures of real-world autobiographical memory retrieval," *Journal of cognitive neuroscience*, vol. 28, no. 4, pp. 604–620, 2016.
- [37] A. M. Gordon, J. Rissman, R. Kiani, and A. D. Wagner, "Cortical Reinstatement Mediates the Relationship Between Content-Specific Encoding Activity and Subsequent Recollection Decisions," *Cerebral Cortex*, vol. 24, pp. 3350–3364, 08 2013.
- [38] J. D. Johnson and M. D. Rugg, "Recollection and the Reinstatement of Encoding-Related Cortical Activity," *Cerebral Cortex*, vol. 17, pp. 2507–2515, 01 2007.
- [39] A. M. Gordon, J. Rissman, R. Kiani, and A. D. Wagner, "Cortical Reinstatement Mediates the Relationship Between Content-Specific Encoding Activity and Subsequent Recollection Decisions," *Cerebral Cortex*, vol. 24, pp. 3350–3364, 08 2013.
- [40] J. Johnson, G. McDuff, M. Rugg, and K. Norman, "Recollection, familiarity, and cortical reinstatement: A multivoxel pattern analysis," *Neuron*, vol. 63, pp. 697–708, 09 2009.
- [41] M. Ritchey, E. Wing, K. LaBar, and R. Cabeza, "Neural similarity between encoding and retrieval is related to memory via hippocampal interactions," *Cerebral cortex (New York, N.Y. : 1991)*, vol. 23, 09 2012.
- [42] H.-Y. S. Chien, H. Goh, C. M. Sandino, and J. Y. Cheng, "Maeeg: Masked auto-encoder for EEG representation learning," 2022. Preprint, arXiv:2211.02625.
- [43] N. Hollenstein, C. Renggli, B. Glaus, M. Barrett, M. Troendle, N. Langer, and C. Zhang, "Decoding EEG brain activity for multi-modal natural language processing," *Frontiers in Human Neuroscience*, vol. 15, 2021.
- [44] J. Żygierewicz, R. A. Janik, I. T. Podolak, A. Drozd, U. Malinowska, M. Poziomska, J. Wojciechowski, P. Ogniewski, P. Niedbalski, I. Terczynska, *et al.*, "Decoding working memory-related information from repeated psychophysiological EEG experiments using convolutional and contrastive neural networks," *Journal of Neural Engineering*, vol. 19, no. 4, p. 046053, 2022.
- [45] S.-Y. Han, N.-S. Kwak, T. Oh, and S.-W. Lee, "Classification of pilots' mental states using a multimodal deep learning network," *Biocybernetics and Biomedical Engineering*, vol. 40, no. 1, pp. 324–336, 2020.
- [46] M. N. Mohsenvand, M. R. Izadi, and P. Maes, "Contrastive representation learning for electroencephalogram classification," in *Machine Learning for Health*, pp. 238–253, PMLR, 2020.
- [47] H. Banville, O. Chehab, A. Hyvärinen, D.-A. Engemann, and A. Gramfort, "Uncovering the structure of clinical EEG signals with self-supervised learning," *Journal of Neural Engineering*, vol. 18, no. 4, p. 046020, 2021.
- [48] V. J. Lawhern, A. J. Solon, N. R. Waytowich, S. M. Gordon, C. P. Hung, and B. J. Lance, "Eegnet: a compact convolutional neural network for EEG-based brain-computer interfaces," *Journal of neural engineering*, vol. 15, no. 5, p. 056013, 2018.
- [49] U. R. Acharya, H. Fujita, S. L. Oh, Y. Hagiwara, J. H. Tan, M. Adam, and R. S. Tan, "Deep convolutional neural network for the automated diagnosis of congestive heart failure using ECG signals," *Applied Intelligence*, vol. 49, no. 1, pp. 16–27, 2019.
- [50] S. Lee and J.-H. Chang, "Oscillometric blood pressure estimation based on deep learning," *IEEE Transactions on Industrial Informatics*, vol. 13, no. 2, pp. 461–472, 2017.
- [51] M. van Gerven, J. Farquhar, R. Schaefer, R. Vlek, J. Geuze, A. Nijholt, N. Ramsey, P. Haselager, L. Vuurpijl, S. Gielen, and P. Desain, "The brain-computer interface cycle," *Journal of neural engineering*, vol. 6, p. 041001, 09 2009.
- [52] L. M. Ward, "Synchronous neural oscillations and cognitive processes," *Trends in Cognitive Sciences*, vol. 7, no. 12, pp. 553–559, 2003.

- [53] A. K. E. Markus Siegel, Tobias H. Donner, “Spectral fingerprints of large-scale neuronal interactions,” *Nature Reviews Neuroscience*, vol. 13, no. 2, pp. 121–134, 2012.
- [54] W. Klimesch, “Alpha-band oscillations, attention, and controlled access to stored information,” *Trends in Cognitive Sciences*, vol. 16, no. 12, pp. 606–617, 2012.
- [55] T. Harmony, T. Fernández, J. Silva, J. Bosch, P. Valdés, A. Fernández-Bouzas, L. Galán, E. Aubert, and D. Rodríguez, “Do specific EEG frequencies indicate different processes during mental calculation?,” *Neuroscience Letters*, vol. 266, no. 1, pp. 25–28, 1999.
- [56] K. Allan and M. Rugg, “An event-related potential study of explicit memory on tests of cued recall and recognition,” *Neuropsychologia*, vol. 35, no. 4, pp. 387–397, 1997.
- [57] J. A. Meltzer, M. Negishi, L. C. Mayes, and R. T. Constable, “Individual differences in EEG theta and alpha dynamics during working memory correlate with fmri responses across subjects,” *Clinical Neurophysiology*, vol. 118, no. 11, pp. 2419–2436, 2007.
- [58] Wikipedia, “Wikipedia, the free encyclopedia,” 2010.
- [59] X. Lei and K. Liao, “Understanding the influences of EEG reference: A large-scale brain network perspective,” *Frontiers in Neuroscience*, vol. 11, p. 205, 2017.
- [60] S. A. Hillyard and L. Anllo-Vento, “Event-related brain potentials in the study of visual selective attention,” *Proceedings of the National Academy of Sciences*, vol. 95, no. 3, pp. 781–787, 1998.
- [61] Y. Bengio, A. Courville, and P. Vincent, “Representation learning: A review and new perspectives,” *IEEE transactions on pattern analysis and machine intelligence*, vol. 35, no. 8, pp. 1798–1828, 2013.
- [62] G. Florian and G. Pfurtscheller, “Dynamic spectral analysis of event-related EEG data,” *Electroencephalography and Clinical Neurophysiology*, vol. 95, no. 5, pp. 393–396, 1995.
- [63] S. M. Zoldi, A. Krystal, and H. S. Greenside, “Stationarity and redundancy of multichannel EEG data recorded during generalized tonic-clonic seizures,” *Brain Topography*, vol. 12, no. 3, pp. 187–200, 2000.
- [64] F. T. Liu, K. M. Ting, and Z.-H. Zhou, “Isolation forest,” in *2008 Eighth IEEE International Conference on Data Mining*, pp. 413–422, 2008.
- [65] P. Khosla, P. Teterwak, C. Wang, A. Sarna, Y. Tian, P. Isola, A. Maschinot, C. Liu, and D. Krishnan, “Supervised contrastive learning,” *Advances in neural information processing systems*, vol. 33, pp. 18661–18673, 2020.
- [66] K. Salama, “Supervised contrastive learning.” <https://keras.io/examples/vision/supervised-contrastive-learning/>, November 2020.
- [67] T. Tieleman and G. Hinton, “Rmsprop.” Lecture slides, 2012.
- [68] L. Van der Maaten and G. Hinton, “Visualizing data using t-SNE.,” *Journal of machine learning research*, vol. 9, no. 11, 2008.
- [69] J. T. Devlin, R. P. Russell, M. H. Davis, C. J. Price, H. E. Moss, M. J. Fadili, and L. K. Tyler, “Is there an anatomical basis for category-specificity? semantic memory studies in pet and fmri,” *Neuropsychologia*, vol. 40, no. 1, pp. 54–75, 2002.
- [70] J. D. E. Gabrieli, R. A. Poldrack, and J. E. Desmond, “The role of left prefrontal cortex in language and memory,” *Proceedings of the National Academy of Sciences*, vol. 95, no. 3, pp. 906–913, 1998.
- [71] C. Pallier, A.-D. Devauchelle, and S. Dehaene, “Cortical representation of the constituent structure of sentences,” *Proceedings of the National Academy of Sciences*, vol. 108, no. 6, pp. 2522–2527, 2011.
- [72] J. R. Binder, C. F. Westbury, K. A. McKiernan, E. T. Possing, and D. A. Medler, “Distinct brain systems for processing concrete and abstract concepts,” *Journal of cognitive neuroscience*, vol. 17, no. 6, pp. 905–917, 2005.
- [73] M. Oberhuber, T. M. H. Hope, M. L. Seghier, O. Parker Jones, S. Prejawa, D. W. Green, and C. J. Price, “Four Functionally Distinct Regions in the Left Supramarginal Gyrus Support Word Processing,” *Cerebral Cortex*, vol. 26, pp. 4212–4226, 10 2016.
- [74] E. K. Miller and J. D. Cohen, “An integrative theory of prefrontal cortex function,” *Annual Review of Neuroscience*, vol. 24, no. 1, pp. 167–202, 2001. PMID: 11283309.
- [75] G. Liakakis, J. Nickel, and R. Seitz, “Diversity of the inferior frontal gyrus—a meta-analysis of neuroimaging studies,” *Behavioural Brain Research*, vol. 225, no. 1, pp. 341–347, 2011.

- [76] M. Reilly, N. Machado, and S. Blumstein, "Hemispheric lateralization of semantic feature distinctiveness," *Neuropsychologia*, vol. 75, pp. 99–108, 2015.
- [77] C. Mummery, K. Patterson, R. Wise, R. Vandenberghe, C. Price, and J. Hodges, "Disrupted temporal lobe connections in semantic dementia," *Brain : a journal of neurology*, vol. 122 (Pt 1), p. 61–73, January 1999.
- [78] A. Martin and L. L. Chao, "Semantic memory and the brain: structure and processes," *Current Opinion in Neurobiology*, vol. 11, no. 2, pp. 194–201, 2001.
- [79] A. J. Golby, R. A. Poldrack, J. B. Brewer, D. Spencer, J. E. Desmond, A. P. Aron, and J. D. E. Gabrieli, "Material-specific lateralization in the medial temporal lobe and prefrontal cortex during memory encoding," *Brain*, vol. 124, pp. 1841–1854, 09 2001.
- [80] J. Fell, P. Klaver, H. Elfadil, C. Schaller, C. Elger, and G. Fernández, "Rhinal-hippocampal theta coherence during declarative memory formation: Interaction with gamma synchronization?," *The European journal of neuroscience*, vol. 17, pp. 1082–8, 04 2003.
- [81] G. G. Knyazev, "EEG delta oscillations as a correlate of basic homeostatic and motivational processes," *Neuroscience & Biobehavioral Reviews*, vol. 36, no. 1, pp. 677–695, 2012.
- [82] T. Fernandez, T. Harmony, J. Gersenowies, J. Silva-Pereyra, F.-B. A, G. L, and D.-C. L., "Sources of EEG activity during a verbal working memory task in adults and children," in *Advances in Clinical Neurophysiology* (R. Reisin, M. Nuwer, M. Hallett, and C. Medina, eds.), vol. 54 of *Supplements to Clinical Neurophysiology*, pp. 269–283, Elsevier, 01 2002.
- [83] S. Hanouneh, H. U. Amin, M. N. Mohamad Saad, and A. Malik, "Eeg power and functional connectivity correlates with semantic long-term memory retrieval," *IEEE Access*, vol. PP, pp. 1–1, 01 2018.
- [84] S. Hanslmayr, T. Staudigl, and M.-C. Fellner, "Oscillatory power decreases and long-term memory: the information via desynchronization hypothesis," *Frontiers in Human Neuroscience*, vol. 6, 2012.
- [85] L. R. Squire, L. Genzel, J. T. Wixted, and R. G. Morris, "Memory consolidation," *Cold Spring Harbor perspectives in biology*, vol. 7, no. 8, p. a021766, 2015.
- [86] R. R. Selvaraju, M. Cogswell, A. Das, R. Vedantam, D. Parikh, and D. Batra, "Grad-cam: Visual explanations from deep networks via gradient-based localization," in *Proceedings of the IEEE International Conference on Computer Vision*, pp. 618–626, 2017.
- [87] S. Debener, R. Emkes, M. De Vos, and M. Bleichner, "Unobtrusive ambulatory EEG using a smartphone and flexible printed electrodes around the ear," *Scientific reports*, vol. 5, no. 1, p. 16743, 2015.

Appendix A. Wikipedia topics

Set 6 Urban Planning, Alan Greenspan, Tamils, Trojan Horse, Deep Sea Exploration, Neolithic

Set 7 Sea Breeze, Dublin, Scientific Method, Garage Rock

Set 8 Bojack Horseman

Set 9 AI Winter

Set 10 Quagga, Norval Morrisseau, Moonlanding Conspiracy, Brownsville, Kabuki, Candlepin Bowling, House of Faberge, Rwanda, Pine, Nelson Mandela

Set 11 Noh, Appropriation, Finland

Set 12 Korean Idol, Computer Algebra, Christopher Wren, Carson City Nevada

Set 13 Bronze Age, Perennial Plant, University of Calgary, Populism, William Tweed, White Blood Cells, Booker Prize, Raul Julia, New Delhi, Premier League

Set 14 Algebraic Structure, Private Equity, Surf Culture, Optical Illusion, Kimono, Maglev, Monopoly, James K Polk, Copenhagen, Plant Communication

Set 15 Betty Ford, Coal In China, Inorganic Chemistry, Optical Transistor, Close Up Magic, Euphrates, Tornado, Sieve of Emtostheves, Leo Tolstoy

Set 16 Power Plant, US Census Bureau, Abraham Flexner, Megadiverse Countries, Environmental Migrant

Set 17 Burrell Collection, Caveat Emptor, Cuban Missile Conflict, Dante Alighieri, Donald Knuth, Jacinda Arden, Nigeria, Pinball, Trans Canada Highway, Walkman Effect

Set 19 Chicago Tribune, Dhaka, Everglades, International Court Of Justice, Joan Didion, Language Death, Miguel De Cervantes, Nihilism, Rhino Entertainment, Sister City

Set 20 The Green Revolution, Lake Victoria, Calligraphy, Marx Brothers, Vandals, Gravity Assist, Thomas Lipton, Amaranth, Samoa, Vavilov Center

Set 21 Nuremberg, Seven Years War, Atoll, Trackball, Liz Clairborne, Uluru, Hass Avocado, Folate, Tessellation, Carlo Gambino